The Effects of Non-line of Sight (NLOS) Channel on a User with Varying Device Orientations

Shakir Ullah(✉), Saeed Ur Rehman, and Peter Han Joo Chong

Department of Electrical and Electronic Engineering,
Auckland University of Technology, Auckland, New Zealand
{shakir.ullah, saeed.rehman, peter.chong}@aut.ac.nz

Abstract. Recently, there has been a growing interest in visible light communications (VLC) for indoor communication to meet the ever-increasing data demands. Most of the studies have considered the line-of-sight (LOS) channel for VLC communication. However, the LOS gain is constrained as the user moves away from the transmitter (Tx) or his device experiences orientation changes. It is observed in practice, the gain from reflections along the defused/NLOS channels can also contribute to optical gain. This research work, therefore, analytical model the NLOS channels and user's device orientation and analyze its effect on the user's SNR. For simulations, analytical models are integrated into ns3. Our results show that SNR slightly improves, which can be utilized to keep the communication alive during the high mobility scenario that could arise due to device orientation.

Keywords: VLC · NLOS · VLC channel · Mobile VLC

1 Introduction

In recent years the visible light communication (VLC) (operates in the frequency range 430 to 750 THz) has been explored as a complementary interference-free spectrum to RF spectrum for providing data communication. VLC offers a broad spectrum and, therefore, can meet the growing spectrum demand with high data rates to the end-users [1]. Apart from the additional spectrum, the VLC has the added advantage of having a readily available infrastructure in the form of light-emitting diodes (LEDs) at homes and other indoor establishments, making it cost-effective. The VLC uses unlicensed frequency band, and thus, there are no current legal restrictions involving bandwidth allocation. Also, VLC is inherently secure as light cannot penetrate walls, and hence, its communication can be restricted to a specific area which allows it to be used for secure communication in the indoor environment. In recent research articles, the VLC system is looked upon as a potential candidate for the beyond 5G and 6G communication system [2, 3].

The VLC offers many advantages in the context of indoor communication; however, most of its optical gain comes from the LOS channel. In the LOS arrangement the transmitter (Tx) and the receiver (Rx) are required to be directed at each other, and thus

J. Zheng et al. (Eds.): ADHOCNETS 2019, LNICST 306, pp. 241–251, 2019.
https://doi.org/10.1007/978-3-030-37262-0_20

the channel gain depends on the angle of emission (AOE) of the Tx, the angle of incidence (AOI) at the Rx, and the Rx field of view (FOV). Of all these factors, AOI is of critical importance as it depends on the user device orientation and can be a constraining factor on received gain. If the user device is in LOS with Tx, that is its photodetector (PD) is facing in the direction of Tx; the AOI is not a limiting factor and the received gain in maximum. However, in practical scenarios, the receiver orientation changes and as a result, it varies its AOI, which in turn cause variations in the SNR performance.

Although most of the VLC gain is from the LOS channel, however, in reality, the light emitted from Tx does not travel in a perfect beam, but instead many of its rays get scattered in different directions across the room. These rays are reflected to the user device after striking the defused surfaces such as walls, ceilings, or other objects in the room, thus forming a defused or non-line of sight (NLOS) channel. These NLOS/defused channels contribute to the optical gain at the receiver, which can be useful for a mobile user.

The presence of NLOS channels necessitates its modeling and the analysis of its effects on VLC users. In the context of indoor VLC research, the channel modeling and optimization of SNR performance is of significant interests. In [4], VLC's LOS and NLOS channels are modeled using neural networks and based on the proposed model; practical experiments are performed to determine the number of taps required for the channel. The intended model use as input parameters such as reflection coefficients of different materials, noise levels, the Rx gain, and the distance between Tx and Rx. This work considers mobile user only in terms of movement inside the room while the user device orientation changes and its effects on Rx gain are not taken into considerations. Similarly, Miramirkhani *et al.,* in [5], have modeled VLC channel for a mobile user, and based on the proposed model, the power profile as well as the delay spread, are determined at different positions for a random mobile user. This work is, however, not taking into considerations the effect of the NLOS channels on mobile users.

User mobility is mostly considered only in terms of user movement, ignoring changes in device orientation. In [6], experimental work is carried out for multi-input and multi-output (MIMO) VLC systems to increase user data rates. In [7], the authors have implemented the theoretical concepts of VLC in MATLAB for short-range 4x4 MIMO systems. However, MIMO systems are evaluated for LOS arrangement of static users. The user device orientation changes and its effect on the received optical gain have attracted some research. In [8], an access point (AP) selection algorithm is developed, which uses the signal strength and user data rates as an input parameter. This approach considers the user device orientation and its effect on data rates. This study examines both the LOS and NLOS channels; however, the impact of different reflections on mobile user performance is not studied. In [9], authors have optimized bit error rate (BER) performance for different SNR scenario by adjusting the tilting mobile user plane. In [10], the BER and outage probability relationship is derived for a mobile user from the statistical distribution of VLC downlink. In [11], the effects of random receiver orientation (for polar and azimuth variations) on LOS channel gain is studied. However, these works have not considered the NLOS channel during the VLC system modeling. NLOS channel can provide an increase optical gain, which can of help during the device tilting.

Most of the existing work has considered the LOS channel for static users. In some of the studies, the user's device orientation is also taken into considerations. However, these studies do not report the effects of NLOS communication on the user's devices, particularly for orientation changes. In this research work, we analytically model the NLOS channels and orientation changes and then analyze the gain from the defused reflections on mobile users. To evaluate these models, we have developed an ns3 simulation tool based on the VLC open-source module [12].

In Sect. 2, we analytical model the VLC channel. In Sect. 3, we model the user device orientation for arbitrary rotations. In Sect. 4, we discuss the performance evaluation metrics. In Sect. 5, we discuss the simulation setup. The results from the experiments are discussed in Sect. 6, and Sect. 7 concludes the paper.

2 Analytical Modeling of VLC Systems

In the VLC systems, as shown in Fig. 1, the current generated from the LED/laser diode (LD) in the Tx is modulated by the information signal I(*t*), which varies the intensity of the source optical signal *x*(*t*). At the Rx, the photodetector (PD) generates photocurrent directly proportional to the incident optical signal on it.

The transmitted VLC signal travels through the VLC channel, modeled as a linear system according to Eq. (1) [13].

$$y(t) = Rx(t) \oplus h(t) + n(t) \tag{1}$$

Where $y(t)$ represents the output photocurrent, R is the PD's responsivity, $h(t)$ is the channel impulse response, and $n(t)$, represents the noise. The noise sources are the result of interference from the shot and the thermal noise. The channel response can be divided into LOS and NLOS gains, discussed later in details.

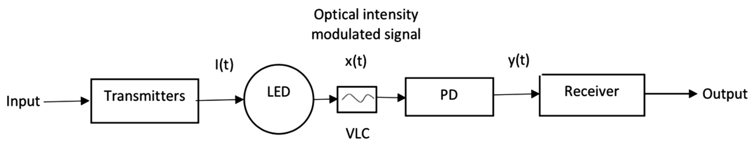

Fig. 1. VLC system main components [13]

2.1 LOS Channel Modeling

In the VLC systems, the photocurrent and incident (instantaneous) optical signal are in direct proportions, and thus it represents a power signal. For this reason, two constraints are imposed on the transmitted signal: (1) the signal must be non-negative, and (2) the transmitted power must be in the range to meet the eye safety as well as minimum illumination requirements. These constraints demand that power must be limited to some constant factor P_{MAX} and by implications the x(t).

The transmitted signals in VLC are real and positive, and thus, the relationship between them can be easily derived with direct current (DC) gain from the VLC channels as below in Eq. (2).

$$P_{Rx} = (H(0) + H(0)_{NLOS})P_{Tx} \quad (2)$$

where P_{Rx} is the power received at Rx, P_{Tx} is the transmitted signal power, the H(0) and $H(0)_{NLOS}$, represents the DC gain from the LOS and NLOS channel (discussed later in Sect. 2.2), respectively. The LOS channel gain can be expressed using Eq. (3) [18] as represented in Fig. 2.

$$H(0) = \frac{(m_l + 1)A}{2\pi d^2} cos^{m_l}(\emptyset) T_s g(\psi)\cos(\psi) \quad (3)$$

Where A is the PD area (m^2), d is the distance between Tx and Rx, and T_s, is the Tx gain. The m_l represents the Lambertian order given as $-ln(2)/ln(2)\cos(\Phi_{1/2})$, where $\Phi_{1/2}$, represents the Tx semi angle at half transmit power. The $g(\psi)$, represents the optical concentrator gain, which can be calculated according to Eq. (3.13) [13], and $\emptyset$ represents the angle of emission at Tx, which, in most of the studies, is considered fixed on the ceiling. The cos (ψ) represents the gain from AOI at the Rx. As we consider user device to experience orientation changes and, therefore, change the AOI which can in turn vary the Rx gain. The AOI gain can be given in Eq. (4) as the ratio of the dot product of the Tx and Rx, the distance d, with the device normal n_r, and the distance norm, $||d||$.

$$\cos\psi = \frac{d.n_r}{||d||} \quad (4)$$

2.2 Non-LOS Channel Modeling

In addition to the parameters from Eq. (3), the NLOS gain calculations needs the room dimensions, walls and ceilings surface areas, the colour of material surfaces, and positioning of the Tx as well as Rx. The Rx power is defined in Eq. (5) [13, 14] (Fig. 2 shows the LOS and NLOS channel model):

$$P_{r-NLOS} = \left(\sum_R H_{NLOS}(0)\right)P_t \quad (5)$$

Where P_{r-NLOS} is the received power from all the NLOS channels and is calculated by integrating all the components after reaching Rx. The reflected light can undergo different orders of reflections, and as a result, could cover different distances. This phenomenon can lead to broadening of the pulse, which can ultimately result in a reduction of signal bandwidth.

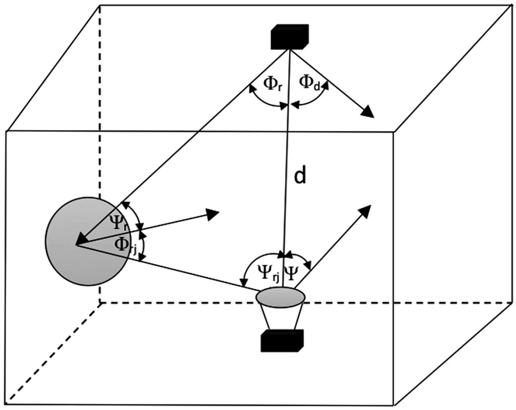

Fig. 2. VLC channel model including LOS and NLOS channels

However, the higher-order reflections contribute less to the optical gain because of larger distance covered and are thus the dominant factor in broadening the pulse. On the other hand, the first-order reflections are dominant contributors to the optical gain and cover less distance while arriving simultaneously. The authors in [15] have used the same observations and considered only first-order reflections in an additive manner with the LOS gain. To measure the effects of first-order reflections, the walls of the room are divided into R reflecting elements; each one has area ΔA. Further, each NLOS channel can be divided into two components. The first component is from transmitting source to a point on the wall (or any other object in the room), acting as a point receiver. The second component is from the point on the walls (acting as a point source) reflecting light, using the Lambertian emission pattern, to the receiver device scaled by walls reflectivity coefficient, p. Using this understanding the impulse response of NLOS channel can thus be represented as below in Eq. (6):

$$H_{NLOS} = \sum_{j=1}^{R} \frac{(m_l + 1)p\Delta A}{2\pi d_{S,j}^2 d_{R,j}^2} cos^{m_l}\left(Q_{Sj}\right) \cos\left(\Psi_{Sj}\right) \cos\left(\Psi_{Rj}\right) \tag{6}$$

Where $d_{S,j}$ is the distance from the Tx to the wall point, $d_{R,j}$, represents the distance point source to the Rx, and R represents the number of reflectance sources. The values for these parameters are specified in Table 1.

3 Receiver Orientation Modelling

In most studies, the user device's PD is considered static in a LOS arrangement, which gives maximum gain. However, in practical scenarios, mobile devices change their orientation frequently, which affects the SNR from the LOS channels, and consequently affects the data rates, and quality of service (QoS). Modern mobile devices are equipped with components such as gyroscope, and accelerometer, to measure their motion and rotations in 3D. A 3D rotation about an arbitrary point is composed of three rotations, along with x,y and z coordinates [16], represented as in Eq. (7):

$$\mathrm{R} = R_x(\alpha)R_y(\beta)R_z(\gamma) \tag{7}$$

These rotations are yaw, pitch, and roll angles, represented by α, β, γ, respectively. The α represents rotation around z-axis, and it can take values from 0 to 360°; β, represents rotation around x-axis, which is tipping device towards and away, and can gain value from −180 to 180°; and γ, represents rotation around y-axis and represents device rotation from left to right and can take values from −90 to 90°. When the user device is static, the normal vector of the PD, n_r [0; 0; 1] ^{T}, is given below in Eq. (8) [8].

$$n_r = R(\alpha, \beta, \gamma) \tag{8}$$

However, after the rotation of the device, the unit normal vector experience rotation changes as given by Eq. (9) [8]:

$$n_r^{/} = \begin{bmatrix} \sin\alpha\sin\beta\cos\gamma + \cos\alpha\sin\gamma \\ \sin\alpha\sin\gamma - \cos\alpha\sin\gamma\cos\beta \\ \cos\beta\cos\gamma \end{bmatrix} \tag{9}$$

After filling this value in Eq. (4), we get the angle of incidence angle at receiver.

4 Performance Evaluation Metric

The proposed VLC system performance is measured in terms of SNR, which is proportional to the square of the received optical power signal. The Eq. (10) expresses the relationship between SNR, the Rx power, and the total noise. We consider noise only from ambient light sources and thermal noise in the Tx and Rx.

$$SNR = \frac{(P_r R)^2}{\sigma_{total}^2} \tag{10}$$

Where P_r denotes the average received optical power of the signal, is the responsivity of the photodetector and σ_{total}^2 is the total noise variance. In VLC the overall noise is the sum of shot and thermal noise Eq. (11) [12]:

$$\sigma_{total}^2 = \sigma_{shot}^2 + \sigma_{thermal}^2 \tag{11}$$

Based on [12, 17], the shot and thermal noise can be calculated in Eqs. (12) and (13):

$$\sigma_{shot}^2 = 2_q PRB + 2_q I_2 I_b B \tag{12}$$

$$\sigma_{thermal}^2 = \frac{8\pi k T_k}{G_{ol}} C_{pd} A I_2 B^2 + \frac{16\pi^2 k T_k n}{g_n} C_{pd}^2 A^2 I_3 B^3 \tag{13}$$

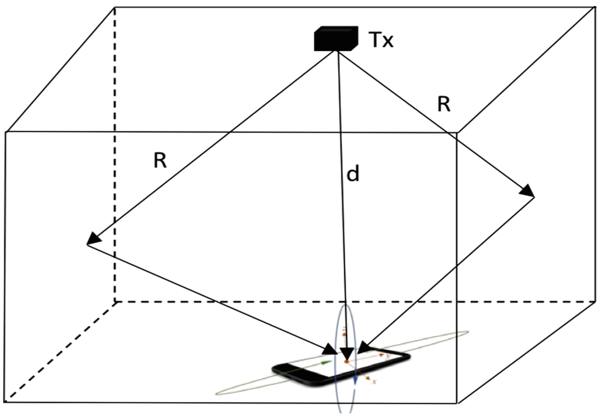

Fig. 3. Simulation setup for ns3 simulator

Where B is the bandwidth of PD, k is the Boltzmann's constant, I_b is the photocurrent due to background radiations, G_{ol} is the voltage gain, T_k is the absolute temperature, C_{pd} is the capacitance per unit area, I_2 and I_3, represents the noise bandwidth factor values. The values used for simulation is provided in Table 1.

5 Simulation Results

To evaluate our proposed model, we have created a scenario in ns3, which consists of a Tx and an Rx, in a room of $5 \times 5 \times 5$ dimensions, as shown in Fig. 3. The Tx is fixed in the roof facing downwards, and Rx is a user device with orientation changes, modeled as discussed in Sect. 3. Further, the walls of the room are considered of plaster, with reflectivity 0.8 [13]. We have used static routing to enforce packets flow in the network, simulated with 1 Mbps of data, where each packet is of 1040 size. We have carried out three types of simulations for evaluating the effects of NLOS channels on VLC user's performance.

In the first scenario, the LOS channel is simulated for a static user according to the parameters shown in Table 1. In the second scenario, the gains from NLOS channels are added to the LOS channel, and the combined channel is evaluated for a user with static device orientation. In the third simulation scenario, the LOS and NLOS channels are combined for a dynamic user, which experiences device orientation changes. In our simulations, we have kept alpha α at 0 and beta (β) varies between -180 to 180. These two parameters show rotation around z-axis and y-axis. The rotation around x is represented by gamma (γ) and varies from -90 to 90. The results are arranged according to the reflectance factor of the wall materials [13]. The parameters for simulations are listed in Table 1 based on [13] and [12].

Table 1. Simulation parameters

Parameter	Value
Lambertian Order Semiangle, Φ1/2	70°
Filter Gain, Ts	1
Boltzmann's constant, k	1.3806e−23 J/K
Noise bandwidth factor, I2	0.562
Background current IB	5100−6 A
Open-loop voltage gain, Gol	10
Fixed capacitance of photo, Cpd	112pF/cm2
Field-effect transistor (FET) transconductance (gm)	30 ms
electronic charge, q	1.60217e−19 C
I3	0.0868
Photo Detector Area, A	1.0e−4 m2
Refractive Index, n	1.5
field of view, ψcon	70○
Transmitter coordinate	(0.0,0.0,50.0)
Receiver coordinate	(0.0,0.0, dist)
α	0.85,0.60
Bandwidth factor, B	10
Distance, d	50 m
Absolute temperature, Tk	295
Reflectance coefficient	0.8
Reflectance Areas	0.28
Dimensions	5,5,5
Temperature, T	5000
FET channel noise factor, Γ	1.5
Modulation Scheme	OOK

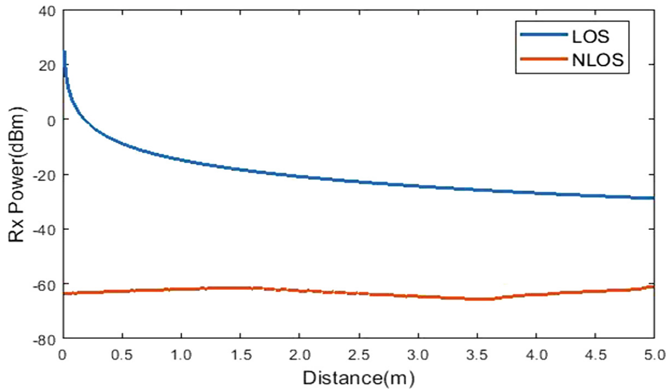

Fig. 4. Received power from LOS only, and combined LOS and NLOS combined channels

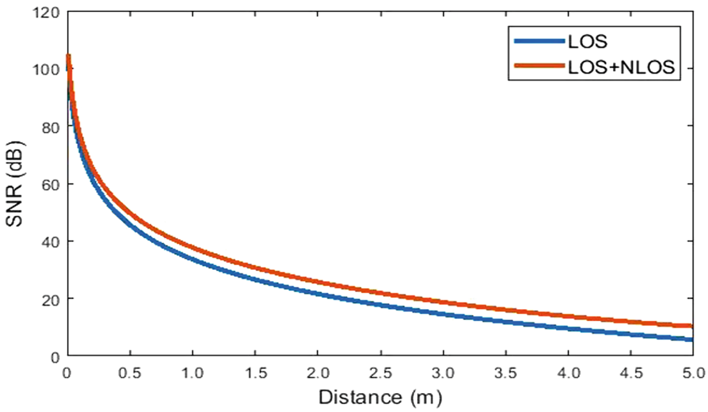

Fig. 5. SNR from LOS only, and combined LOS and NLOS channels when the user device orientation is static

6 Results Discussion

The Rx optical gain, as a function of the distance between Tx and Rx, from the LOS and NLOS channel is shown in Fig. 4. The results show, the gain from the LOS channel is high, but it decreases as the user moves away from Tx, and for NLOS channels, the gain is less but consistent. In Fig. 5, the SNR for combined LOS and NLOS shows improvement over the LOS only channel.

Apart from the above simulations where Rx moves away from the Tx with static device orientation, we have also carried simulations for scenarios where user device experiences orientation changes. The user device orientation is modeled according to Sect. 3. Figure 6 shows a slight improvement of SNR of combined channel over LOS only, specifically when the distance from the Tx increases

From these simulations, it can be observed that user device gets optimum gain from LOS channel up to a certain distance from Tx, and with static orientation. However, when user device moves away from Tx or experiences orientation changes, the VLC SNR performance starts to degrade. On the other hand, when we combine both the channels, the SNR improves. This is very important as in most practical scenarios the user devices are away from Tx and can experience low optical gain from the LOS channel. Similarly, when the user device experience orientation changes the LOS gain suffer as shown Fig. 6, and the VLC gain improves.

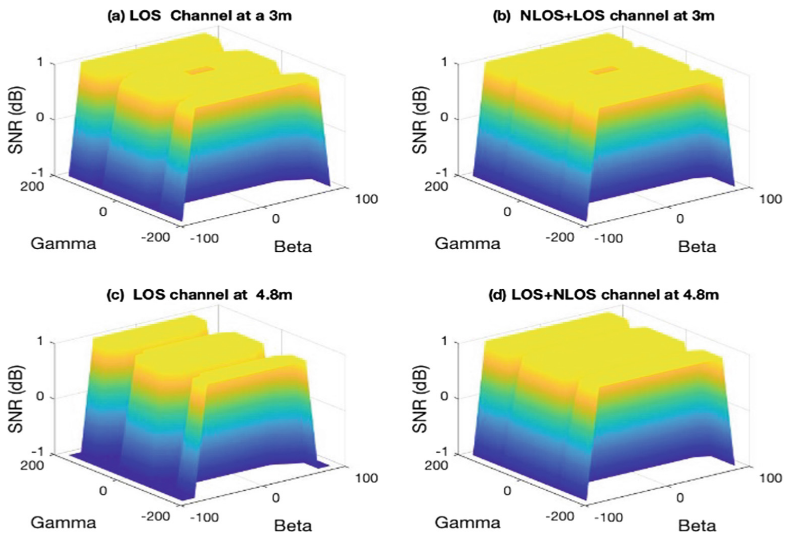

Fig. 6. SNR for LOS and NLOS channel for user device experiencing orientation changes

7 Conclusions

The VLC is coined as a new physical medium for future generation wireless network i.e., beyond 5G and 6G. Existing literature mostly focused on the LOS channel for data communication due to the physics of LED light. However, when the user moves away from Tx or his device orientation changes the receiver gain is drastically affected due to the user movement or orientation changes. This makes the gain from the NLOS/defused channels more critical. Based on our simulation for LOS and combined channel, we have demonstrated that NLOS gain can have a positive effect on the SNR performance and could be a source of communication during the mobile scenario either due to user movement or change in orientation. Building on the existing analysis, our future work would consider the full channel implementation (LOS and NLOS alike) to model the BER and goodput for a mobile scenario and developing algorithms to consider the changes in the handover in a heterogenous environment.

References

1. Turan, B., Narmanlioglu, O., Ergen, S.C., Uysal, M.: Physical layer implementation of standard compliant vehicular VLC. In: Vehicular Technology Conference (VTC-Fall) IEEE 84th, pp. 1–5. IEEE (2016)
2. Strinati, E., Barbarossa, S., Luis Gonzalez-Jimenez, J., Ktenas, D., Cassiau, N., Dehos, C.: 6G: The Next Frontier (2019)
3. Syed, J.N., Sharma, S.K., Wyne, S., Patwary, M., Asaduzzaman, M.: Quantum machine learning for 6G communication networks: State-of-the-Art and vision for the future, pp. 46317–46350 (2019)

4. Dong, Z., Shang, T., Gao, Y., Li, Q.: Study on VLC channel modeling under random shadowing. IEEE Photonics J. **9**(6), 1–16 (2017)
5. Miramirkhani, F., Narmanlioglu, O., Uysal, M., Panayirci, E.: A mobile channel model for VLC and application to adaptive system design. IEEE Commun. Lett. **21**(5), 1035–1038 (2017)
6. Rajbhandari, S., et al.: Neural network-based joint spatial and temporal equalization for MIMO-VLC system. IEEE Photonics Technol. Lett. **31**(11), 821–824 (2019)
7. Amsdon, T., Sibley, M.J.: Theoretical concepts and matlab modelling of VLC based MIMO systems, University of Huddersfield (2013)
8. Soltani, M.D., Wu, X., Safari, M., Haas, H.: Access point selection in Li-Fi cellular networks with arbitrary receiver orientation. In: 2016 IEEE 27th Annual International Symposium on Personal, Indoor, and Mobile Radio Communications (PIMRC), pp. 1–6 (2016)
9. Wang, J., et al.: Improvement of BER performance by tilting receiver plane for indoor visible light communications with input-dependent noise. In: 2017 IEEE International Conference on Communications (ICC), pp. 1–6 (2017)
10. Eroglu, Y., Yapici, Y., Guvenc, I.: Impact of random receiver orientation on visible light communications channel. IEEE Trans. Commun. **67**(2), 1313–1325 (2017)
11. Dehghani Soltani, M., Andi Purwita, A., Tavakkolnia, I., Haas, H., Safari, M.: Impact of device orientation on error performance of LiFi systems. IEEE Access **7**, 41690–41701 (2018)
12. Aldalbahi, A., et al.: Extending ns3 to simulate visible light communication at network-level. In: 2016 23rd International Conference on Telecommunications (ICT), pp. 1–6. IEEE (2016)
13. Ghassemlooy, Z., Popoola, W., Rajbhandari, S.: Optical Wireless Communications: System and Channel Modelling with MATLAB (2012)
14. Kahn, J.M., Barry, J.R.: Wireless infrared communication **85**(2), 265–298 (1997)
15. Wu, X., Safari, M., Haas, H.: Access point selection for hybrid Li-Fi and Wi-Fi networks. IEEE Trans. Commun. **65**(12), 5375–5385 (2017)
16. Huynh, D.Q.: Metrics for 3D rotations: Comparison and analysis. J. Math. Imaging Vis. **35**(2), 155–164 (2009)
17. Dimitrov, S., Haas, H.: Principles of LED Light Communications: Towards Networked Li-Fi. Cambridge University Press, Cambridge (2015)